Composites Science and Technology 89 (2013) 98–109

Contents lists available at ScienceDirect

Composites Science and Technology

journal homepage: www.elsevier.com/locate/compscitech

Brittle matrix composites with heterogeneous reinforcement: Multi-scale model of a crack bridge with rigid matrix

R. Rypl [a,*], R. Chudoba [a], A. Scholzen [a], M. Vořechovský [b]

[a] Institute of Structural Concrete, RWTH Aachen University, Germany
[b] Institute of Structural Mechanics, Brno University of Technology, Czech Republic

ARTICLE INFO

Article history:
Received 23 April 2013
Received in revised form 21 August 2013
Accepted 21 September 2013
Available online 5 October 2013

Keywords:
A. Ceramic–matrix composites (CMCs)
B. Strength
B. Stress/strain curves
C. Multiscale modeling
C. Statistics

ABSTRACT

A mechanical multi-scale model describing the relationship between the crack-opening and composite bridging stress in brittle matrix composites with heterogeneous reinforcement is introduced. Unlike currently utilized models, it is able to reflect the heterogeneity of fibrous reinforcement. Mechanical, geometrical and bond properties of individual fibers (e.g. fiber surface roughness, radius, strength) are defined as random variables. The functional dependency between these random variables and the fiber stress within the composite cross-section is introduced using local equilibrium equations. The response of the composite to an applied uniaxial tensile load is evaluated by averaging the fiber stress contributions in a crack bridge.

In particular, the model describes the behavior of a single crack bridge in a composite assuming the matrix to be rigid. The fiber bridging action is represented using the shear-lag model. Upon fiber rupture the global load sharing for stress redistribution is considered. With these assumptions the rules for asymptotic Daniels' fiber-bundle models can be applied for the evaluation of macroscopic crack bridge behavior. We use the model to illuminate the effect of selected sources of heterogeneity (fiber breaking strain, fiber radius and bond strength) on the crack bridge response and to approximately predict the ultimate state of a multiply cracked composite. The model constitutes a basis for the multi-scale simulation of the strain-hardening response of brittle-matrix composites.

1. Introduction

The combination of brittle matrix (ceramic, cementitious) with fibrous reinforcement provides the possibility to design composites with tuned properties, in particular with a favorable quasi-ductile behavior and high load bearing capacity [34,9]. When loaded in tension, brittle matrix composites exhibit multiple cracks developing in the matrix perpendicularly to the loading direction over a range of applied stresses up to a state of crack saturation and ultimately localized failure within the weakest crack bridge [25,15,1,2,21,7,8,32]. This process is accompanied by damage evolution and significant stress redistribution both between and within the constituents of the composite [27,47,42,29,10,22,24]. The qualitative and quantitative characteristics of composites depend on the mechanical, geometrical and statistical properties of the constituents and their interface [51,48]. In a cracked composite, fibers bridge matrix cracks and transmit the applied load into the matrix over a debonded length a which is (in addition to the load) a function of the frictional bond strength τ and fiber radius r [6,26,1,20]. In the case of heterogeneous reinforcement, the debonded length is a random variable, hence the mean fiber strain is nonlinear both with respect to the distance from a crack z and across the crack plane. This phenomenon causes a reduction of the composite strength, which was also observed experimentally [46].

We introduce a mechanical multi-scale single crack bridge model that incorporates reinforcement heterogeneity in the form of statistical distributions of the fiber and bond properties. In particular, we extend our previous work [44,4], which was focused on modeling the tensile behavior of high-modulus multi-filament yarns subjected to tensile loading, by considering the fiber–matrix interface and analyze the effects of its scatter on the crack bridge behavior. In addition, we perform a thorough analysis of fiber fracture location. The homogenization is then performed using the statistical fiber-bundle model [11,5,33]. A similar approach was applied in [43,25,23] where statistical averaging was used for the homogenization of the response of short fibers with random orientation and position. In [13] the homogenized elastic composite properties are obtained by means of Monte Carlo simulation.

The present paper is organized as follows: First, the computational model is introduced generally and assumptions are listed

* Corresponding author. Tel.: +49 (0)241/80 25 172; fax: +49 (0)241/80 22 335.
E-mail address: rrypl@imb.rwth-aachen.de (R. Rypl).

0266-3538/$ - see front matter © 2013 Elsevier Ltd. All rights reserved.
http://dx.doi.org/10.1016/j.compscitech.2013.09.014

in Section 2. Particular applications of the model for three random variables are described in Section 3 and validation is provided in Section 4. Finally, conclusions are drawn and related issues are briefly discussed in Section 5.

2. Computational model

2.1. Assumptions and notation

A unidirectional composite with constant cross-sectional area containing fibers of volume fraction V_f is considered. The fibers exhibit linear elastic behavior with the modulus of elasticity E_f and brittle failure upon reaching their breaking strain. The fiber cross-section is assumed circular with radius r. We neglect the elastic deformation of the matrix and assume it to be rigid. This is justified for cross sections with much higher matrix stiffness compared to the stiffness of the reinforcement $E_m(1 - V_f) \gg E_f V_f$ (E_m – matrix modulus of elasticity).

Matrix cracks in a composite subjected to tensile load are assumed to be planar and perpendicular to the loading direction. Any residual force transferred by the matrix crack planes is neglected so that the force is transmitted solely by the fibers. When the tensile load is increased, fibers debond and constant bond stress τ acts at the interface over the debonded length a (Fig. 1). It is further assumed that the distance between cracks is large enough so that the debonded lengths of individual fibers do not overlap and crack bridges can be considered as mechanically independent.

Although detailed analyzes of stress profiles within a fiber cross section have been performed in the past [27,49,50], we assume the stress concentrations at the fiber perimeter close to the matrix crack plane to have a minor effect (see also [9]) and use the fundamental assumption of shear-lag models [27] of constant fiber stress over the cross-section. Nevertheless, the stress is variable for individual fibers due to the parameters which affect the fiber–matrix bond and which are assumed to be of random nature. The mechanical idealization of the composite can thus be described as a parallel set of independent 1D springs representing the fibers coupled to a rigid body representing the matrix through a (possibly random) frictional bond.

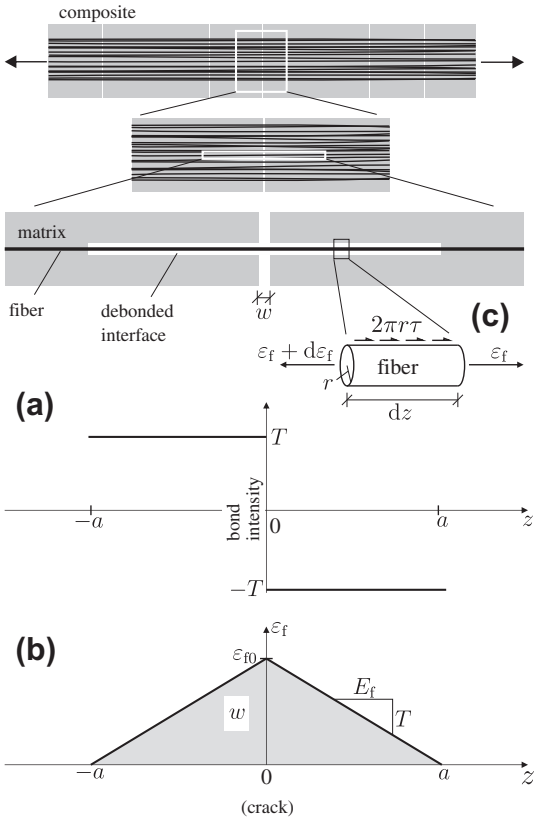

Fig. 1. (a) Bond intensity $T(z)$ given by Eq. (2); (b) fiber strain $\varepsilon_f(z)$ given by Eq. (4); (c) differential equilibrium on the fiber.

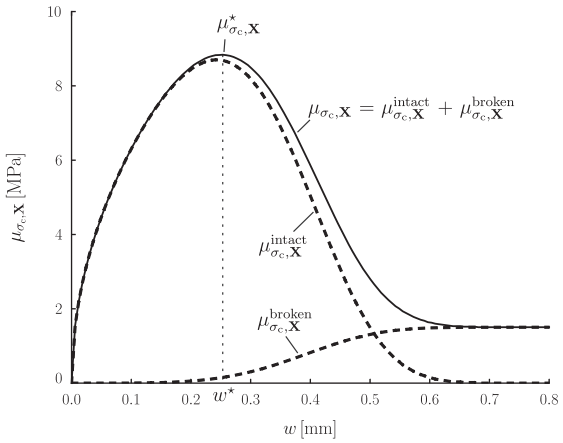

Fig. 2. Typical composite stress vs. crack opening diagram (mean composite function).

The response of the composite crack bridge is represented by the statistical average of the contributions of individual fibers assuming a large number of fibers. Further assumptions applied here follow the rules for Daniels' statistical fiber-bundle models [11,5,36,31,18,39,30] which include global load sharing of the applied load by fibers in proportion to their stiffness and irrespective of their position within the bundle. This is justified for cementitious and most ceramic matrix composites where the bond strength is relatively low and the matrix stiffness relatively high [35,34,9].

Let us note, that for composites with rather strong bond and low matrix stiffness, global load sharing would be a crude simplification. The stress redistribution of broken fibers here follows the local load sharing which was studied analytically in [16,22] for simple fiber packing (linear, square) and later numerically in [47,40] for more complex fiber packing within the cross-section. Statistical models introduced in [9,34] approach the local load sharing by dividing the composite longitudinally and laterally into independent finite-sized sub-bundles satisfying the weakest link features. The composite strength is then evaluated as the minimum extreme of the sub-bundle strength distribution which is approximated by the Gaussian distribution for asymptotic bundles (and adjusted by the shift of the mean value for finite-sized bundles as proposed in [39,12]).

2.2. Single fiber model

Individual fibers in a composite with rigid matrix are mechanically independent and we can therefore define their strain regardless of the strain state of neighboring fibers. When a matrix crack opens, the bridging fibers debond and transmit an amount of force that corresponds to their debonded length and the frictional sliding resistance τ at the fiber–matrix interface. We state the differential equilibrium condition for the debonded fibers at the longitudinal distance from the matrix crack z

$$E_f \frac{d\varepsilon_f(z)}{dz} + T \cdot \mathrm{sign}(z) = 0 \tag{1}$$

where we introduce the longitudinal fiber strain ε_f and the bond intensity T for the debonded part of a fiber defined as the interface shear flow acting on the fiber cross section Fig. 1

$$T = \frac{2\pi r\tau}{\pi r^2} = \frac{2\tau}{r}. \tag{2}$$

The fiber strain derivative for the debonded range of a fiber with respect to the longitudinal position z is thus

$$\frac{d\varepsilon_f(z)}{dz} = -\frac{T}{E_f}\,\mathrm{sign}(z). \tag{3}$$

If we analyze the fiber strain profile along the crack bridge, the maximum is found at the crack plane $z = 0$ and with growing distance from the crack the function decays linearly with the slope $-T/E_f$ until it reaches zero at $z = \pm a$. An explicit expression for the fiber strain can be obtained by integrating Section 3.2

$$\varepsilon_f(z) = \begin{cases} \int_{-a}^{z} \frac{d\varepsilon_f(x)}{dx}\,dx = \frac{T[a - z\cdot\mathrm{sign}(z)]}{E_f} & : z \in (-a, a) \\ 0 & : \text{otherwise.} \end{cases} \tag{4}$$

The maximum strain ε_{f0} is obtained by integrating Section 3.2.

$$\varepsilon_{f0} = \varepsilon_f(0) = \int_{-a}^{0} \frac{d\varepsilon_f(z)}{dz}\,dz = \frac{Ta}{E_f}. \tag{5}$$

The crack opening w is obtained by integrating ε_f over the whole debonded domain as

$$w = \int_{-a}^{a} \varepsilon_f(z)\,dz = \frac{Ta^2}{E_f}. \tag{6}$$

If the substitution $a = \varepsilon_{f0}E_f/T$ from Eq. (5) is performed, the maximum fiber strain can be directly defined as a function of w

$$\varepsilon_{f0}(w) = \sqrt{\frac{Tw}{E_f}}. \tag{7}$$

We now introduce the effect of fiber rupture. The fiber strain value ε_{f0} at which the fiber fails shall be denoted as ξ and we refer to it as the fiber breaking strain. We can thus define the strain of an intact fiber at a crack plane in combination with the Heaviside step function as

$$\varepsilon_{f0,\xi}^{\text{intact}} = \varepsilon_{f0}\cdot H(\xi - \varepsilon_{f0}) \tag{8}$$

where $H(\cdot)$ denotes the Heaviside step function defined as

$$H(x) = \begin{cases} 0 & : x < 0 \\ 1 & : x \geqslant 0 \end{cases} \tag{9}$$

As pointed out by various authors studying the ultimate strength of composites [35,49,41,9,34], intact fibers transmit the stress $E_f\varepsilon_{f0}$ and upon breakage at a nonzero distance ℓ from the crack the fiber is still able to transmit residual stress while being pulled out of the matrix. The residual stress transmitted by broken fibers equals the bond intensity T acting on the fiber length ℓ which is being pulled out from the matrix. Some authors subtract the crack opening from the pull-out length [41]. We ignore this effect with the justification that only a small w/ℓ ratio is of practical interest. The strain contribution of broken fibers is thus

$$\varepsilon_{f0,\xi}^{\text{broken}} = \frac{T}{E_f}\ell\cdot H(\varepsilon_{f0} - \xi). \tag{10}$$

Since the distance of the position of the fiber rupture from the crack plane ℓ is a random variable [28,41] and its contribution to the crack bridging force is linear, we can assume it to be represented by its expectation μ_ℓ (see Appendix A for derivation) given by

$$\mu_\ell = \frac{a_\xi}{m+1} \tag{11}$$

where a_ξ is the debonded length at the instant of fiber rupture

$$a_\xi = \xi E_f/T. \tag{12}$$

and m is the Weibull modulus of the fiber strength distribution. Substituting μ_ℓ into Eq. (10) then gives

$$\varepsilon_{f0,\xi}^{\text{broken}} = \frac{\xi}{m+1}\cdot H(\varepsilon_{f0} - \xi) \tag{13}$$

and the total strain of a fiber during the loading process is the addition of the two parts

$$\varepsilon_{f0,\xi}(w) = \varepsilon_{f0,\xi}^{\text{intact}} + \varepsilon_{f0,\xi}^{\text{broken}}. \tag{14}$$

In [34], the author refers to this kind of load sharing between intact and broken fibers as 'frictional load sharing'.

2.3. Stress homogenization and composite stress

As is the case with the strain-based bundle models [33,4], we use the (quasi-static) crack opening w as a kinematic control variable that is identical for all fibers within the crack bridge irrespective of their local stress state. The behavior of the crack bridge is studied assuming randomness in fiber breaking strain ξ and in parameters affecting the bond strength – r and τ (E_f is taken to be deterministic).

In what follows, we introduce the homogenization procedure and derive the general formula for the mean, homogenized composite stress in a crack bridge[1] $\mu_{\sigma_c,\mathbf{X}}(w,\mathbf{X})$ as a function of the crack opening and a general vector of random variables $\mathbf{X}$. The function $\mu_{\sigma_c,\mathbf{X}}(w,\mathbf{X})$ will be referred to as the 'mean composite function' further in the text. In Section 3 particular evaluations of the mean composite function are shown.

The composite stress σ_c is, by definition, the sum of fiber forces $f_{f,i}$ transmitted by all n_f fibers within a crack plane divided by the composite cross-sectional area A_c.

$$\sigma_c = \frac{1}{A_c}\sum_{i=1}^{n_f} f_{f,i}(w,\mathbf{X}). \tag{15}$$

Let us remark, that $f_{f,i}$ is a function of the crack opening w and of the random vector $\mathbf{X}$. The explicit notation of these dependencies is omitted in the following formulas. Assuming a large number of fibers, we can define $\sum_{i=1}^{n_f} f_{f,i}$ and A_c in terms of expected values stating that

$$\sum_{i=1}^{n_f} f_{f,i} \approx n_f \mathrm{E}[f_f] \tag{16}$$

and

$$A_c \approx n_f \frac{\mathrm{E}[A_f]}{V_f} \tag{17}$$

where $A_f = \pi r^2$ is the single fiber cross-sectional area. Substituting Eqs. (16) and (17) into Eq. (15) and assuming fibers exhibit linear elastic behavior ($f_{f,i} = E_f\varepsilon_{f0,\xi}A_f$), we write the mean composite function μ_{σ_c} (with the w dependency omitted)

$$\sigma_c \approx \mu_{\sigma_c} = V_f\frac{\mathrm{E}[f_f]}{\mathrm{E}[A_f]} = V_f\frac{\mathrm{E}[E_f\varepsilon_{f0,\xi}A_f]}{\mathrm{E}[A_f]} = E_f V_f \mathrm{E}\left[\varepsilon_{f0,\xi}\frac{A_f}{\mathrm{E}[A_f]}\right]. \tag{18}$$

We further define the dimensionless fiber cross-section which is the fraction in the square brackets in Eq. (18), thus

$$v_f(r) = \frac{A_f}{\mathrm{E}[A_f]} = \frac{r^2}{\mathrm{E}[r^2]} \tag{19}$$

[1] Remark on notation: Mean values are denoted μ with a subscript indicating the random function and a list of random variables. For example $\mu_{\sigma_c\mathbf{X}}$ is the mean value of the random function σ_c which depends on the random variables $\mathbf{X}$.

and finally write the general form

$$\mu_{\sigma_c}(w,\mathbf{X}) = E_f V_f \mathrm{E}\left[\varepsilon_{f0,\xi}(w,\mathbf{X}) v_f(r)\right]. \tag{20}$$

The maximum of the mean composite function Eq. (20) shall be referred to as the mean composite strength and is defined as

$$\mu^{\star}_{\sigma_c}(\mathbf{X}) = \sup\{\mu_{\sigma_c}(w,\mathbf{X}); w \geqslant 0\}. \tag{21}$$

When computing the mean composite function, the main task is the evaluation of the expectation $\mathrm{E}[\varepsilon_{f0,\xi}(w) v_f(r)]$ using $\varepsilon_{f0,\xi}(w)$ as defined in Eq. (14).

3. Analysis of random effects

The following paragraphs report on systematically performed parametric studies with combinations of random and deterministic parameters. The studies reveal the correspondence between the individual sources of randomness and the response of a crack bridged by heterogeneous reinforcement. If the properties of all fibers in the composite are deterministic, the mean composite function Eq. (20) is simply

$$\mu_{\sigma_c}(w) = \sigma_c(w) = E_f V_f \varepsilon_{f0,\xi}(w) \tag{22}$$

Here, the strain, which is identical for all fibers, is multiplied by the fiber stiffness. Note that for deterministic fiber radius r, the dimensionless cross-section $v_f(r)$ defined by Eq. (19) becomes 1.

3.1. Random fiber breaking strain ξ

Most authors studying the mechanical properties of fiber reinforced composites assume the fiber strength to be the only source of randomness [39,35,22,17,41,38,9]. We use the fiber-in-composite breaking strain distribution, which was also used in the above mentioned references (see Appendix C for full derivation), in the two parameter Weibull form

$$G_\xi(\xi) = 1 - \exp\left[-\left(\frac{\xi}{\varepsilon_0}\right)^{m+1}\right] \tag{23}$$

with the scale parameter

$$\varepsilon_0 = \left(\frac{T(m+1)\varepsilon_{V_0}^m V_0}{2E_f \pi r^2}\right)^{1/(m+1)} \tag{24}$$

and the corresponding density function

$$g_\xi(\xi) = \frac{\partial G_\xi(\xi)}{\partial \xi} = \frac{m+1}{\varepsilon_0}\left(\frac{\xi}{\varepsilon_0}\right)^m [1 - G_\xi(\xi)]. \tag{25}$$

Let us note that ε_0 is related to the normalizing scale parameter σ_c used e.g. in [20,9] as $\varepsilon_0 = (m+1)^{1/(m+1)}\sigma_c$. In our study, however, it would be of little benefit to use this normalization since τ and r (and consequently also the normalizing scale) are random variables.

3.1.1. Stress homogenization for random fiber breaking strain

Having derived the density function g_ξ, we can use it to evaluate the mean composite function with random fiber breaking strain in the following manner

$$\mu_{\sigma_{c,\xi}}(w) = E_f V_f v_f(r) \int_0^\infty \varepsilon_{f0,\xi}(w,\xi) g_\xi(\xi) \mathrm{d}\xi. \tag{26}$$

In analogy to Eq. (14) we split the homogenization of the composite stress into contributions from intact and broken fibers (see Fig. 2). Recalling that $v_f(r) = 1$ for deterministic fiber radius, the first term within the homogenization procedure, corresponding to intact fibers, becomes

$$\begin{aligned}\mu^{\mathrm{intact}}_{\sigma_{c,\xi}}(w) &= E_f V_f \varepsilon_{f0} \int_0^\infty H(\xi - \varepsilon_{f0}) g_\xi(\xi) \mathrm{d}\xi \\ &= E_f V_f \varepsilon_{f0} \int_{\varepsilon_{f0}}^\infty g_\xi(\xi) \mathrm{d}\xi = E_f V_f \varepsilon_{f0}[1 - G_\xi(\varepsilon_{f0})]\end{aligned} \tag{27}$$

and the second term, corresponding to broken fibers, becomes (with the use of Eqs. (16) and (17))

$$\begin{aligned}\mu^{\mathrm{broken}}_{\sigma_{c,\xi}}(w) &= TV_f \int_0^\infty \mu_\ell H(\varepsilon_{f0} - \xi) g_\xi(\xi) \mathrm{d}\xi \\ &= \frac{E_f V_f}{m+1} \int_0^{\varepsilon_{f0}} \xi g_\xi(\xi) \mathrm{d}\xi.\end{aligned} \tag{28}$$

The integral in Eq. (28) can be solved analytically [41]

$$I_\xi(\varepsilon_{f0}) = \int_0^{\varepsilon_{f0}} \xi g_\xi(\xi) \mathrm{d}\xi = \varepsilon_0 \cdot \gamma\left(1 + \frac{1}{m+1}, \left[\frac{\varepsilon_{f0}}{\varepsilon_0}\right]^{m+1}\right) \tag{29}$$

with γ standing for the lower incomplete gamma function. Note that in [35,34,9] the contribution of broken fibers is well approximated by simpler formulas. The resulting form of the homogenized composite stress with random fiber breaking strain is then with regard to the dependency $\varepsilon_{f0}(w)$ given in Eq. (28)

$$\begin{aligned}\mu_{\sigma_{c,\xi}}(w) &= \mu^{\mathrm{intact}}_{\sigma_{c,\xi}}(w) + \mu^{\mathrm{broken}}_{\sigma_{c,\xi}}(w) \\ &= E_f V_f \left[\varepsilon_{f0}[1 - G_\xi(\varepsilon_{f0})] + \frac{I_\xi(\varepsilon_{f0})}{m+1}\right].\end{aligned} \tag{30}$$

After all fibers have broken (i.e. for large values of w), the first term in Eq. (30) representing intact fibers is zero and the second term representing the residual stress transmitted by the pull-out of broken fibers is

$$\mu_{\sigma_{c,\xi}}(w \to \infty) = \mu^{\mathrm{broken}}_{\sigma_{c,\xi}}(w \to \infty) = E_f V_f \frac{I_\xi(w \to \infty)}{m+1} \tag{31}$$

with

$$I_\xi(w \to \infty) = \varepsilon_0 \cdot \Gamma\left(\frac{1}{m+1}\right) \tag{32}$$

where Γ denotes the complete gamma function.

Numerical evaluations of Eq. (30) are shown in Fig. 3 in the bottom diagram for three values of the Weibull modulus m. The corresponding breaking strain distributions are depicted in the upper diagram. They are normalized in such a way that the mean value of ξ is constant for all three distributions. Higher values of m denoting narrow distributions of fiber breaking strain result in more brittle behavior being exhibited by the composite crack with a higher ultimate stress. Residual stresses transmitted by the pull-out of intact fibers are higher for lower m because fibers with a high variation of breaking strain will in average break further away from the matrix crack.

3.1.2. Composite strength with random fiber breaking strain

Of particular interest is the mean composite strength $\mu^{\star}_{\sigma_c}$ given as the maximum of the composite mean function $\mu_{\sigma_{c,\xi}}(w)$ (Eq. (30)). The corresponding crack opening $w^{\star}$ for which $\mu_{\sigma_{c,\xi}}(w)$ attains its maximum is obtained in the following form (see Appendix B for detailed derivation)

$$\frac{\partial \mu_{\sigma_{c,\xi}}(w)}{\partial w} = 0 \to w^{\star} = \frac{E_f}{T}\varepsilon_0^2 m^{-\frac{2}{m+1}}. \tag{33}$$

Evaluating Eq. (30) for $w^{\star}$ gives the mean composite strength

$$\mu^{\star}_{\sigma_c} = \mu_{\sigma_{c,\xi}}(w^{\star}) = E_f V_f \zeta \cdot \varepsilon_0 \tag{34}$$

with

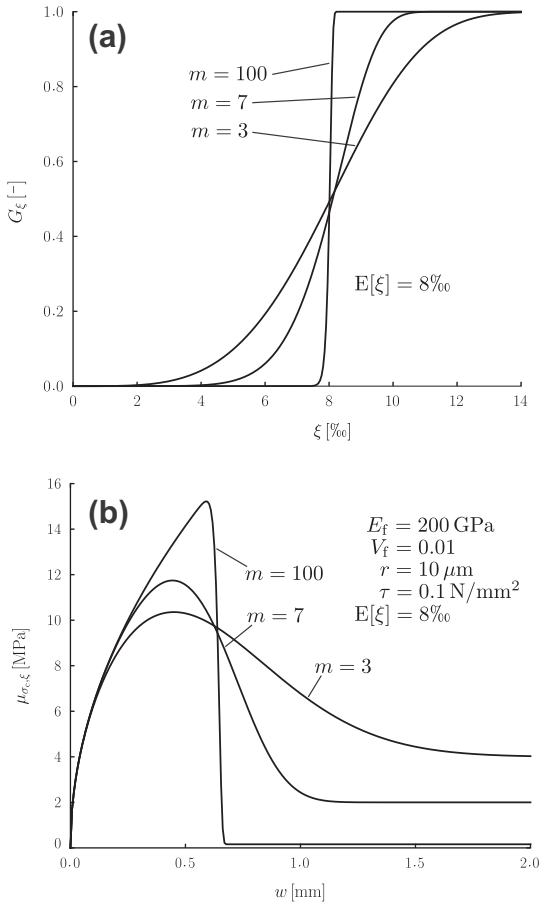

Fig. 3. (a) Fiber breaking strain distribution G_ξ with varying Weibull modulus m and scale parameter adjusted, so that the mean value remains constant; (b) mean composite functions (mean composite stress vs. crack opening) corresponding to the G_ξ in (a).

$$\zeta = \left[m^{-\frac{1}{m+1}} \cdot \exp\left(-\frac{1}{m}\right) + \frac{1}{m+1} \cdot \gamma\left(1 + \frac{1}{m+1}, \frac{1}{m}\right)\right]. \tag{35}$$

Similarly, the fraction of intact fibers at the instant of maximum composite stress is obtained by substituting $w^\star$ from Eq. (33) into Eq. (33)

$$p^\star = 1 - G_\xi[\varepsilon_{f0}(w^\star)] = \exp(-1/m). \tag{36}$$

Let us remark, that this result has been also derived by Daniels [11] and Coleman [5] with their fiber-bundle model describing the behavior of 'dry' bundles (with the absence of matrix) as it is referred to in [14]. We can conclude that the fraction of intact filaments at maximum composite stress remains unaffected even if the bond between filaments and rigid matrix and the pullout of broken fibers are included.

3.2. Interaction of random ξ with random r and τ

In addition to random fiber breaking strain there are various other sources of randomness that cause the reinforcement to behave heterogeneously. In this section, we consider variations of fiber radius r caused by the methods used to produce filaments in multi-filament yarns, and also variations in bond strength τ which are caused e.g. by fiber surface roughness, fiber sizing quality or matrix penetration (Fig. 4). For example in the case of multi-filament yarn reinforcement used in textile reinforced concrete, the variations in the matrix-filament bond are especially pronounced. They are caused by the irregular penetration of the matrix into the yarn and by the micro-structure of the fine grained cement matrix [19]. Statistical dependencies between the variables, which are considered random, may occur. However, within this study we consider these dependencies minor and treat the random variables as statistically independent.

3.2.1. Effect of deterministic r and τ

Before approaching the analysis of the effects of additional random variables on crack bridge response, we consider their influence as deterministic variables.

First, we use Eq. (30) from Section 3.1 to study the effect of deterministic r and τ on the composite mean function. With explicitly denoted dependencies on r and τ, Eq. (30) is written as

$$\mu_{\sigma_{c,\xi}}(w, r, \tau) = E_f V_f [\varepsilon_{f0}(r,\tau)[1 - G_\xi(\varepsilon_{f0}(r,\tau))] + \frac{I_\xi(\varepsilon_{f0}(r,\tau), r, \tau)}{m+1}\Big]. \tag{37}$$

Fig. 5 (upper diagrams) depicts the mean composite functions for various values of r and τ.

The effect of r and τ on the mean composite strength is apparent, if an analysis is made of the behavior of Eq. (34) where the two variables occur in the scale parameter ε_0. Written explicitly, we obtain

$$\mu^\star_{\sigma_{c,\xi}}(r,\tau) = E_f V_f \zeta \left(\frac{\tau(m+1)\varepsilon_{V_0}^m V_0}{E_f \pi r^3}\right)^{1/(m+1)}. \tag{38}$$

Hence the scaling of the mean composite strength with respect to the fiber radius (Fig. 5c) can be expressed as

$$\mu^\star_{\sigma_{c,\xi}}(r) \propto r^{-3/(m+1)} \tag{39}$$

and the scaling with respect to the bond strength as (Fig. 5d)

$$\mu^\star_{\sigma_{c,\xi}}(\tau) \propto \tau^{1/(m+1)} \tag{40}$$

which corresponds to [9]. As it is the case with the mean composite strength, we can study the crack opening at peak composite stress $w^\star$ as a function of the two variables r and τ. For this purpose, we substitute ε_0 from Eq. (24) into Eq. (33) and use the substitution $T = 2\tau/r$ to obtain

$$w^\star_\xi(r,\tau) = \frac{rE_f}{2\tau} m^{-\frac{2}{m+1}} \cdot \left(\frac{\tau(m+1)\varepsilon_{V_0}^m V_0}{E_f \pi r^3}\right)^{2/(m+1)}. \tag{41}$$

Clearly, we can state that

$$w^\star_\xi(r) \propto r^{1-6/(m+1)} \tag{42}$$

and

$$w^\star_\xi(\tau) \propto \tau^{-1/(m+1)}. \tag{43}$$

An interesting conclusion can be drawn, if we observe the scaling of $w^\star_\xi$ with r: If $m = 5.0, w^\star_\xi$ is a constant independent of the fiber radius because the r terms in Eq. (41) cancel out. For $m > 5.0, w^\star_\xi$ grows with growing r and for $m < 5.0$ it decays with growing r; see Fig. 5c. With growing τ, the crack opening at peak stress $w^\star_\xi$ will decay for all values of m; see Fig. 5d.

3.2.2. Effect of random r and τ

The mean composite function for deterministic r and τ given by Eq. (37) can be used to evaluate the mean composite function when r and τ are defined as random variables. We assume that the distribution functions of the random variables G_r and G_τ and their corresponding density functions g_r and g_τ are known. We will first derive the homogenized crack bridge behavior for only a single random variable (in addition to the random fiber breaking strain). The evaluation is performed by integrating the mean

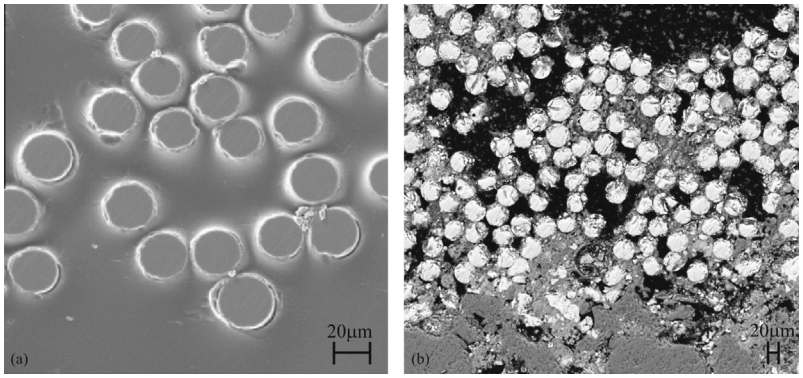

Fig. 4. Micrographs of filaments in matrix provided by the Institute of Textile Technology (ITA) of the RWTH University in Aachen, Germany: detail of scatter in fiber radius r (a); detail of matrix penetration into a multi-filament yarn – source of scatter in bond strength τ (b).

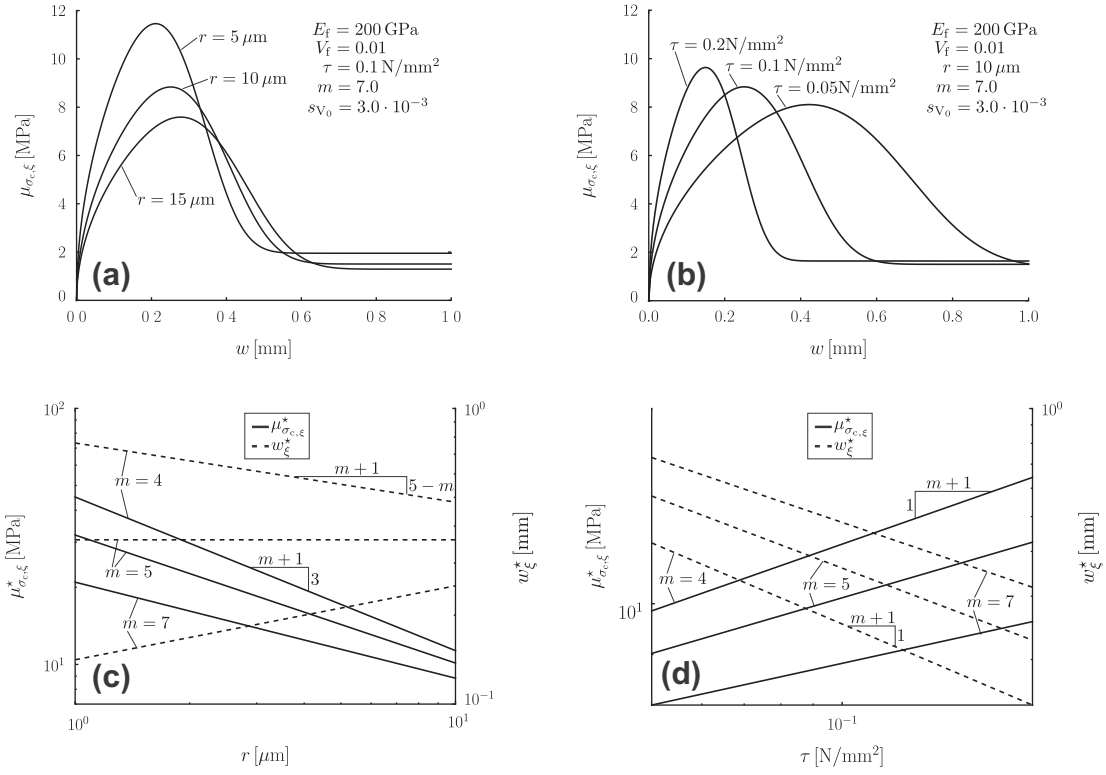

Fig. 5. Effect of deterministic parameters on crack bridge behavior: mean composite function with variable r (a) and τ (b); mean composite strength $\mu^\star_{\sigma_{c,\xi}}$ and crack opening at peak stress $w^\star_\xi$ for variable r (c) and τ (d).

composite function $\mu_{\sigma_{c,\xi}}$ multiplied by the dimensionless fiber radius and the density function g_r or g_τ over the domain of the random variable. In this way the mean composite function for random r is obtained as

$$\mu_{\sigma_{c,\xi r}}(w) = \cancel{E_f V_f} \int_0^\infty v_f(r)\mu_{\sigma_{c,\xi}}(w,r)g_r(r)\mathrm{d}r \tag{44}$$

and for random τ as

$$\mu_{\sigma_{c,\xi\tau}}(w) = \cancel{E_f V_f} \int_0^\infty \mu_{\sigma_{c,\xi}}(w,\tau)g_\tau(\tau)\mathrm{d}\tau. \tag{45}$$

The effect of scatter in filament radius and bond strength on the mean composite strength is quantified using Eqs. (44) and (45), respectively. Three levels of scatter in uniform distribution were applied to show the influence of each random variable (Fig. 6).

It appears that variations in τ and r have a similar qualitative effect on the mean composite strength but the sensitivity of the response with respect to the scatter in the bond strength is somewhat higher. Differences in the influence of the studied variables are found especially in the descending branches of the mean composite functions. Both a lower τ and a higher r reduce the bond intensity T and therefore flatten and prolong the descending branch. However, variations in r additionally affect the fiber breaking strain. Since thicker fibers are more prone to rupture, breakages of fibers with larger radius r and low T are found in earlier loading stages and thus do not substantially contribute to the descending branch. Because of this opposing effect of r, the descending branch remains almost unaffected by the scatter in r.

If scatter in both r and τ is considered at the same time, the mean composite function reads

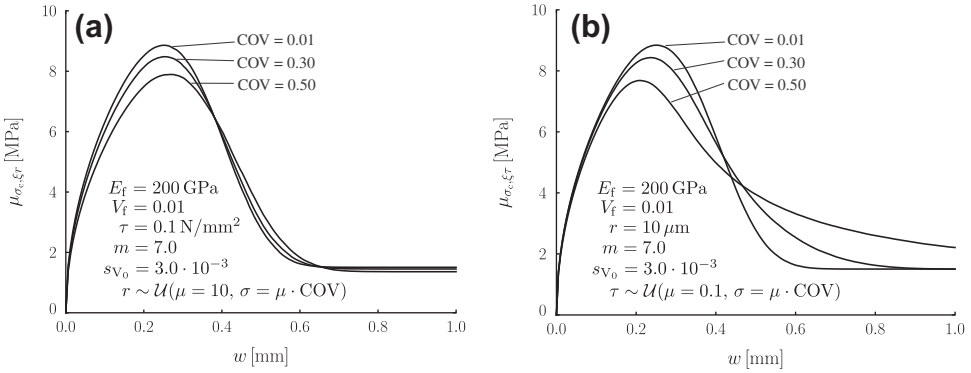

Fig. 6. Mean composite functions (mean composite stress vs. crack opening) for three levels of scatter of the random fiber radius r (a) and bond strength τ (b).

$$\mu_{\sigma_{c,\xi r\tau}}(w) = \cancel{E_f V_f} \int_0^\infty \int_0^\infty v_f(r)\mu_{\sigma_{c,\xi}}(w,r,\tau)g_{r\tau}(r,\tau)\mathrm{d}r\mathrm{d}\tau \tag{46}$$

where $g_{r\tau}(r,\tau)$ is the joint probability density function of the random variables r and τ.

Parametric studies of the mean composite strength $\mu^\star_{\sigma_{c,\xi r\tau}}$ and crack opening at peak stress $w^\star_{\xi r\tau}$ have been performed for various levels of COV of the random variables ξ,r and τ. The sensitivity of $\mu^\star_{\sigma_{c,\xi r\tau}}$ and $w^\star_{\xi r\tau}$ to the scatter in the random variables variables is depicted in Fig. 7 for various m values. Analyzing the results, we can point out the following conclusions:

- Generally, scatter of every considered variable reduces the mean composite strength $\mu^\star_{\sigma_{c,\xi r\tau}}$ since it causes the strain in the fibers to become non-homogeneous.
- The rate of $\mu^\star_{\sigma_{c,\xi r\tau}}$ reduction with scatter in r is faster for smaller values of m.
- The rate of $\mu^\star_{\sigma_{c,\xi r\tau}}$ reduction with scatter in τ is slower for smaller values of m.
- $w^\star_{\xi r\tau}$ decreases with growing scatter in τ and this decreasing tendency is faster for smaller m values.
- $w^\star_{\xi r\tau}$ is unaffected by the scatter in r for $m = 5.0$, which was already explained above.
- For $m > 5.0, w^\star_{\xi r\tau}$ gets reduced with growing scatter in r and for $m < 5.0, w^\star_{\xi r\tau}$ grows with growing scatter in r.

4. Validation of the model

In order to validate the model we introduce the calibration test setup (Section 4.1) and and describe the calibration of parameters using the single crack bridge model (Section 4.2). In Section 4.3, we present the test setup for validation with multiple cracks and in Section 4.4, we provide the appropriate adaptation of the model based on references [34,9,35]. Finally, we discuss the validity of the model in Section 4.5.

Throughout this section we use the fiber stress (and fiber strength – denoted with the ★ superscript) as the mean value $\mu_{\sigma_f} = \mu_{\sigma_c}/V_f$ when referring to model outputs and as force per reinforcement cross-section σ_f when referring to experiments.

4.1. Test setup for calibration

The material used for the experiments was textile reinforced concrete (TRC) which is a composite material with significant bond strength variations due to irregular penetration of matrix into the reinforcing multi-filament yarns. It consists of a fine-grained cementitious matrix which is laminated or sprayed onto carbon textiles [37]. The water-based cementitious matrix does not penetrate the whole cross-section of the multi-filament yarns so that the effective bond strength is variable, see Fig. 4.

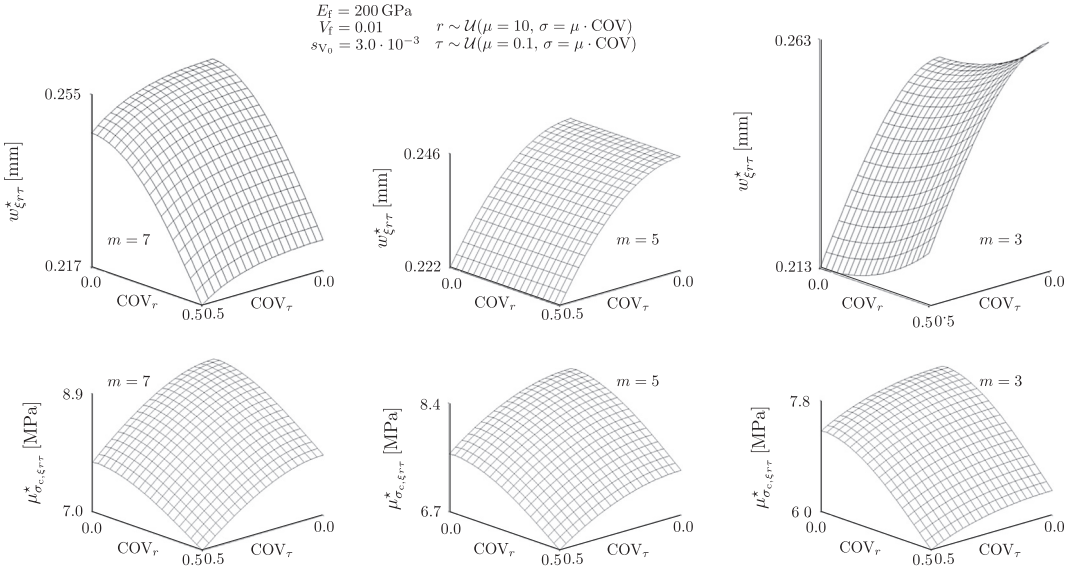

Fig. 7. Crack opening at peak stress (upper diagrams) and mean composite strength (lower diagrams) for random ξ, r and τ.

To match the conditions and assumptions of the single crack bridge model, double sided pullout specimens 40 × 40 × 1000 mm with a single carbon yarn (Toho Tenax Co., Ltd., 12 k, 800 tex) were cast for the purpose of calibration (Fig. 8, left). The ratio of the cross-sectional areas 1600 mm^2 (matrix) and 0.45 mm^2 (yarn) have been chosen to fulfill the high matrix/fibers stiffness ratio $E_m(1 - V_f) \gg E_f V_f$ so that the matrix can be assumed rigid compared to the reinforcement. The length 1000 mm has been chosen in order to reflect the infinite embedded length assumed in the model formulation. In the middle of the specimen's longitudinal axis, a matrix crack was predetermined by a thin steel plate with a round opening in the middle defining the position of the bridging carbon yarn. A mold release agent was used to avoid adhesion of the cementitious matrix to the steel plate (Fig. 8).

A typical test response for a selected specimen is exemplified in terms of σ_f vs. w diagram in Fig. 9. In total, four tests have been conducted with the measured strengths $\sigma_f^\star$ ranging between 805 and 872 MPa with crack openings $w^\star$ between 1.35 and 1.83 mm. The high initial stiffness corresponds to the simultaneous shear stress contribution of all intact fibers in the initial loading stages. The rather long, slowly descending post-peak branch is due to debonding of fibers with a weak bond and the pullout of broken fibers.

4.2. Calibration

If all variables are considered deterministic the developed model has 5 parameters: V_f, E_f, r, ξ, τ. Since the evaluated stresses are related to the actual fiber volume fraction the variable V_f is eliminated. The modulus of elasticity E_f and the filament radius r are assumed to be deterministic with values taken from the producers' specifications: E_f = 240 GPa and r = 3.5 μm. The bond strength τ and fiber breaking strain ξ are considered as random variables.

For ξ, we apply the distribution function G_ξ derived in Appendix C with the typical value of Weibull modulus for dry carbon fibers m = 5.0. As described e.g. in [9] the *in situ* filament breaking strain can be degraded compared to the *ex situ* state so that the scale parameter is a variable for calibration in general. To determine the *in situ* filament strength separately, elaborate fracture mirror analyzes and/or pullout length measurements could provide some help. In the present study, the scale parameter s_{V_0} in G_ξ is to be identified within the calibration. The shape parameter m is assumed equal to the *ex situ* value.

Observing the microscopic structure of a whole yarn cross-section which is partly depicted in Fig. 4, one can distinguish that the majority of filaments in the core of the yarn does not have a direct contact to the matrix. These core filaments only transfer the applied load indirectly due to a rather low friction to neighboring filaments. A much smaller fraction of filaments – sleeve filaments – are fully covered by the matrix around the whole perimeter and will thus have a much stronger bond. A possible distribution function of the effective bond strength reflecting this arrangement is the 3-parameter Weibull distribution with a low shape parameter

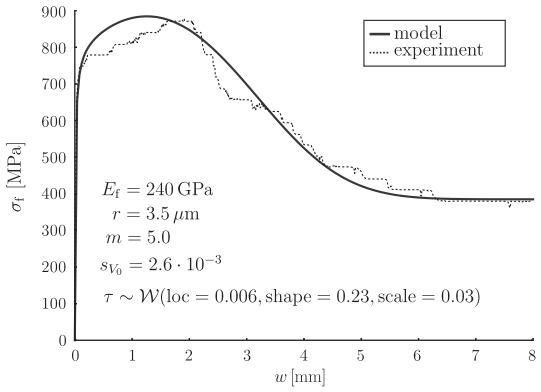

Fig. 9. Typical single crack bridge experimental curve and calibrated single crack bridge model.

(<1.0) which concentrates the majority of the random values at the lower bound. Certainly, other forms of distributions having a similar shape might reflect the bond equally well.

Fig. 9 shows the comparison between the test and the calibrated model. The identified parameters for the applied Weibull distribution for the bond strength τ were: location = 0.006 MPa, scale = 0.03 MPa and shape = 0.23 and the obtained scale parameter of fiber breaking strain scale parameter s_{V0} = 0.0026. Note that with the calibration of a deterministic τ an acceptable fit of the experimental data could not be achieved since it is unable to capture the gradual failure of sleeve and core filaments.

4.3. Test setup for validation

For the validation, dog-bone shaped tensile test specimens with cross-sectional area 100 × 40 mm and gauge length 500 mm were laminated using 12 layers of carbon fabric of the same type as was used for the double sided pullout specimens (Fig. 8, right). In the saturated state the mean crack spacing, measured with the optical 3D measuring machine ARAMIS, was 14 mm with mean crack widths 0.045 mm and the strength $\sigma_f^\star$ was ranging between 1383 and 1496 MPa [37] (in German).

In a multiply cracked specimen, stress and strain profiles are periodic with respect to the individual crack bridges. Consequently, the debonded lengths of the filaments are limited to the half crack spacing distance. This fact introduces a boundary condition that is different from the single crack bridge configuration considered so far. For this situation, the single crack bridge model shall be adapted in order to predict the ultimate state in a multiply cracked specimen.

4.4. Model adaption for periodic boundary conditions

Given the crack spacing l_{CS} of a multiply cracked specimen in the saturated state (Fig. 8) with all fibers fully debonded, fibers

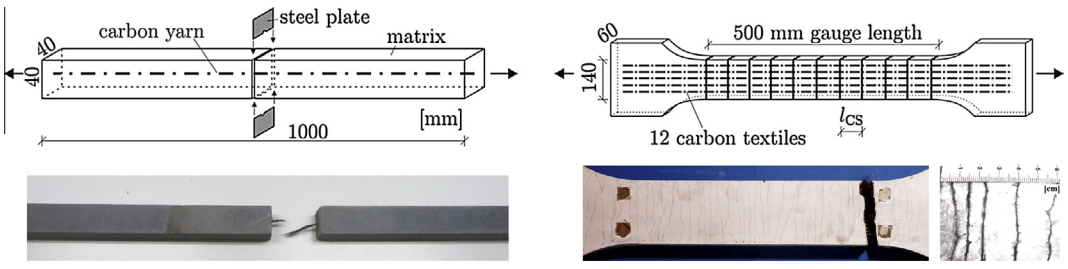

Fig. 8. Single crack bridge tensile specimen (left), multiple cracking tensile specimen (right).

in each crack bridge can be assumed clamped to the matrix at the distance $l_{CS}/2$ from the matrix crack. To include this constraint, the single fiber response (compare with Eq. (7)) has to be modified to take on the linear form

$$\varepsilon_{f0}^{MC}(w) = \frac{w}{l_{CS}} + \frac{T l_{CS}}{4E_f}, \quad \text{for} \quad (a > l_{CS}/2). \tag{47}$$

For the mean pullout length of broken fibers in a multiply cracked composite, we apply the approximation $\mu_\ell \approx a_\xi/2$, which is derived and justified in [34].

To remain consistent with the structure of ε_{f0} derived in Section 2 the strain of a single fiber in a multiply cracked composite at the matrix crack position is divided into the contribution of intact and broken fibers

$$\varepsilon_{f0,\xi}^{MC}(w) = \varepsilon_{f0,\xi}^{MC,intact} + \varepsilon_{f0,\xi}^{MC,broken}. \tag{48}$$

We substitute ε_{f0}^{MC} for ε_{f0} and $a_\xi/2$ for μ_ℓ so that

$$\varepsilon_{f0,\xi}^{MC,intact} = \varepsilon_{f0}^{MC} \cdot H(\xi - \varepsilon_{f0}^{MC}) \tag{49}$$

and

$$\varepsilon_{f0,\xi}^{MC,broken} = \frac{\xi}{2} \cdot H(\varepsilon_{f0}^{MC} - \xi). \tag{50}$$

Further, we follow the common conservative assumption that the fiber strain profile in a multiply cracked composite can be approximated by a constant value [34] as indicated in Fig. 10 so that the fiber breaking strain distribution G_ξ becomes

$$G_\xi^{MC}(\xi) = 1 - \exp\left[-\left(\frac{\xi}{\varepsilon_0}\right)^{m+1}\right] \tag{51}$$

with ε_0 in the form

$$\varepsilon_0 = \left(\frac{T\varepsilon_{V_0}^m V_0}{2E_f \pi r^2}\right)^{1/(m+1)} \tag{52}$$

agreeing with the distribution in [34]. Since both ξ and τ are assumed to be random variables, the variability will be reflected in the strain state of individual fibers. A representative fiber strain is evaluated in terms of statistical average using the procedure described in Section 2 with the derived function for single fiber strain $\varepsilon_{f0,\xi}^{MC}(w)$. Applying G_ξ^{MC} for the fiber breaking strain distribution and

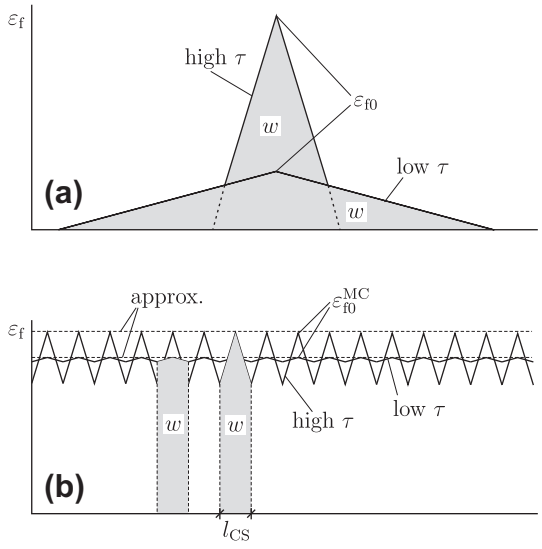

Fig. 10. Schematic strain profiles of two fibers with different τ for single crack bridge (a) multiple cracking (b). The approximated constant strain profile is used for the evaluation of fiber failure probability.

the calibrated 3-parameter Weibull form for the distribution of τ, the mean fiber strength and the corresponding crack opening can be readily computed using Eqs. (20) and (21).

4.5. Discussion

For the calibrated parameters, the adapted crack bridge model predicts the mean fiber strength $\mu_{\sigma_f\xi,\tau} = 1346$ MPa at the crack opening $w^\star_{\xi,\tau} = 0.062$ mm. Compared with dog-bone experiments delivering the strengths 1383–1496 MPa and mean crack opening 0.045 mm [37] the predicted values yield a reasonably good fit although the predicted strength is somewhat lower and the crack opening higher than measured. The underestimation of the strength could be due to the conservative assumption on the fiber strain profile in a multiply cracked composite (Fig. 10) and the overestimation of the crack width due to the rigid matrix assumption and the chosen distribution function for the bond strength τ.

Strength measured on dog-bone specimens with multiple cracks (Fig. 8, right) was more than 50% higher then the strengths of composites with a single crack (Fig. 8, left). The reason for this trend is a homogenization effect on fiber strains in a crack bridge of a multiply cracked composite due to the periodicity of strains along the specimen (Fig. 10).

The differences in fiber strain ε_{f0} due to variations in τ or r (generally T) are most pronounced in case of a single crack bridge where ε_{f0} given by Eq. (7) is proportional to the square root of the crack opening multiplied by T (note the difference in ε_{f0} in Fig. 10a). When the periodic boundary conditions apply (compare the differences in ε_{f0}^{MC} Fig. 10b), the fiber strain close to the ultimate state takes the form Eq. (47) and the variability in ε_{f0}^{MC} is given by the ratio of the constant term $Tl_{CS}/(4E_f)$ involving the variability due to T and the linear term w/l_{CS} independent of T. With growing crack density in the saturated state, i.e. $l_{CS} \to 0$, the first term grows and the second term vanishes. Consequently, the fiber strains approach a constant value independent on the variability in T. This can be viewed as an interaction effect of crack density and scatter in the bond on the crack bridge strength. In simple words, the growing crack density leads to strain homogenization in the fibers in spite of the scatter in the bond intensity and, therefore increases the composite strength.

Another type of interaction effect on composite strength has been identified for crack density and scatter in fiber strength [35,34,9]. In particular, Phoenix and Raj [35] predict strength decrease for the case of multiple cracking due to the higher average fiber strain within the shielded length (Fig. 10b) as compared to the case of a single matrix crack (Fig. 10a). This source of strength reduction is certainly present also in the case of heterogeneous reinforcement. However, for the studied material with high scatter of bond strength the fiber strain homogenization due to increasing crack density described above dominates.

Without claiming that the present study provides a robust validation of the model, we can state that the predicted trends are consistent with the behavior of the tested specimens. Most importantly the adapted crack bridge model for multiple cracking is able to reflect the homogenizing effect of the periodic strain fields.

5. Conclusions

We have provided a framework for evaluating the mean composite stress vs. crack opening function based on a multi-scale mechanical–statistical model of a crack bridge with heterogeneous reinforcement. Variability in virtually every mechanical or geometrical parameter of the fiber and interface properties can be considered within the evaluation and the presented general pattern can be applied for the evaluation of the homogenized composite

response [3]. For demonstration purposes, we have used a simple shear-lag model for fiber pull-out and selected fiber breaking strain, fiber radius and bond strength as examples of random variables.

When analyzing the influence of random fiber breaking strain, we have provided a review of the findings introduced by Oh and Finnie [28] and Evans and Thouless [41] and evaluated scalings of the mean composite strength and crack opening at maximum composite stress which essentially match the results published in [35,9]. Furthermore, when studying the expected value of the pull-out length of broken fibers we came to the conclusion that it equals the debonded length at the instant of the fiber rupture divided by the factor $m + 1$. For AR-glass fibers, for example, $m \approx 5.0$, so the mean pull-out length of fibers would be $\approx 1/6$ of the debonded length corresponding to their breaking strain. Generally, the model documents that with growing variability in fiber breaking strain, the mean composite strength decreases and the failure transits from brittle to ductile (Fig. 3).

If we compare the influence of the parameters r and τ on the crack bridge behavior, two interesting conclusions can be drawn in addition to those described in Section 3.2:

- The crack bridge stiffness in the initial crack opening stages, where all fibers can be assumed intact, is governed by the bond intensity T and fiber modulus of elasticity E_f. Since $T = 2\tau r^{-1}$, the influence of τ on the stiffness is identical to the influence of r^{-1}.
- The mean composite strength scaling with m is, however, not identical for τ and r^{-1}. This can be seen when comparing Eq. (39) and Eq. (40).

The discrepancy between the stiffness and the mean strength scaling is caused by the presence of r^2 in the Weibull scale parameter for fiber breaking strain (see Eq. (24)) which affects the mean composite strength but not the crack bridge stiffness.

The framework of the presented model is also applicable to more complicated fiber (or other bridging element) pull-out models for which the pull-out force against the crack opening is defined by an analytical or numerical relationship provided that the fibers do not interact and their random parameters are identically distributed.

For composites with higher reinforcement ratios, the matrix cannot be assumed rigid and its deformation will influence the fiber stress state. The influence of elastic deformation of the matrix on composite behavior is currently being investigated by the authors. The findings shall be published in a subsequent paper.

Let us emphasize that the presented single crack bridge model was developed as a component of a multi-scale strain hardening model for brittle matrix composites with heterogeneous reinforcement. The description of the whole modeling framework will be provided by the authors in a subsequent paper.

Acknowledgements

This work has been supported by the German Science Foundation under project number CH 276/2-2 and by the Czech Science Foundation (project numbers 13-19416J and FAST-S-13-1889). This support is gratefully acknowledged.

Appendix A. Evaluation of the mean pull-out length

We apply the theory established by Oh and Finnie [28] and used for fiber composites by Evans and Thouless [41] and recall the joint probability density function of fiber failure position within a particular region dL at distance z from the matrix crack and at the reference strain at crack plane ξ

$$h(\xi,z) = (1 - G_\xi)\frac{2m[\xi(1 - z/a_\xi)]^{m-1}}{L_0\varepsilon_0^m}. \tag{A.1}$$

Since the random variables breaking strain ξ and breaking position z are statistically dependent, dividing $h(\xi, z)$ by $g_\xi(\xi)$ (Eq. 25) yields the conditional probability density function of the fracture position, given that the fiber breaks at ξ

$$g_z(z|\xi) = \frac{h(\xi,z)}{g_\xi(\xi)}. \tag{A.2}$$

Note that the terms $(1 - G_\xi)$ cancel and $g_z(z|\xi)$ can be simplified to

$$g_z(z|\xi) = \frac{2m[\xi(1 - z/a_\xi)]^{m-1}}{L_0\varepsilon_0^m}\frac{TL_0}{2E_f}\left(\frac{\varepsilon_0}{\xi}\right)^m = \frac{m}{a_\xi}(1 - z/a_\xi)^{m-1}. \tag{A.3}$$

Density functions $g_z(z|\xi)$ for various values of m are depicted in the left diagram in Fig. A.11. It may seem paradoxical, that for $m < 1$ (dashed line), the fiber breaks are most probable at the very end of the debonded zone, but this can be explained by the form of the hazard rate of the Weibull distribution which, for $m < 1$, is a monotonically decreasing function. Fiber breaks are thus more probable at lower strains – at the end of the debonded zone $z = a$.

To obtain the mean value of the random fracture position given that the fiber break occurs at the strain ξ, Eq. (A.3) is integrated over z

$$\mu_\ell(\xi) = \int_0^{a_\xi} z g_z(z|\xi)\mathrm{d}z = \frac{E_f}{T}\frac{\xi}{m+1} = \frac{a_\xi}{m+1}. \tag{A.4}$$

It might be of interest to evaluate the overall mean pull-out length of all broken fibers at a given crack opening (Fig. A.11), which shall be denoted $\mu_L(w)$. For this purpose, the mean pullout length of individual fibers μ_ℓ has to be integrated over the ξ domain from zero to the ε_{f0} value (corresponding the evaluated crack opening by Eq. 7) and normed with $G_\xi(\varepsilon_{f0})$. The formula then yields

$$\mu_L(w) = \frac{1}{G_\xi(\varepsilon_{f0})}\int_0^{\varepsilon_{f0}} \mu_\ell(\xi) g_\xi(\xi)\mathrm{d}\xi. \tag{A.5}$$

With $a_\xi = \xi E_f/T, \mu_\ell$ can be substituted by $\xi E_f/(T[m + 1])$ resulting in

$$\mu_L(w) = \frac{E_f}{G_\xi(\varepsilon_{f0})T(m+1)}\int_0^{\varepsilon_{f0}} \xi g_\xi(\xi)\mathrm{d}\xi \tag{A.6}$$

which is, using Eq. 7) and

$$\mu_L(w) = \frac{E_f I_\xi(\varepsilon_{f0})}{G_\xi(\varepsilon_{f0})T(m+1)}. \tag{A.7}$$

Appendix B. Evaluation of the crack opening $w^\star$ at the peak of the mean composite function

We use the substitution $k = \sqrt{T/E_f}$ so that $\varepsilon_{f0} = k\sqrt{w}$ and take derivatives of the two summands from Eq. (30) with respect to w. The derivative of the first one $\mu^{\text{intact}}_{\sigma_{c,\xi}}(w)$, is

$$\frac{\partial\mu^{\text{intact}}_{\sigma_{c,\xi}}(w)}{\partial w} = \frac{E_f V_f[1 - G_\xi(k\sqrt{w})]}{2\sqrt{w}}\cdot\left[k - \frac{k^{m+2}(m+1)w^{\frac{m+1}{2}}}{\varepsilon_0^{m+1}}\right] \tag{B.1}$$

and the derivative of the second one $\mu^{\text{broken}}_{\sigma_{c,\xi}}(w)$ is

$$\frac{\partial\mu^{\text{broken}}_{\sigma_{c,\xi}}(w)}{\partial w} = \frac{E_f V_f[1 - G_\xi(k\sqrt{w})]}{2\sqrt{w}}\frac{k^{m+2}w^{\frac{m+1}{2}}}{\varepsilon_0^{m+1}}. \tag{B.2}$$

Setting the sum of the derivatives to zero provides the equation for $w^\star$

$$\frac{\partial\mu^{\text{intact}}_{\sigma_{c,\xi}}(w)}{\partial w} + \frac{\partial\mu^{\text{broken}}_{\sigma_{c,\xi}}(w)}{\partial w} = 0 \tag{B.3}$$

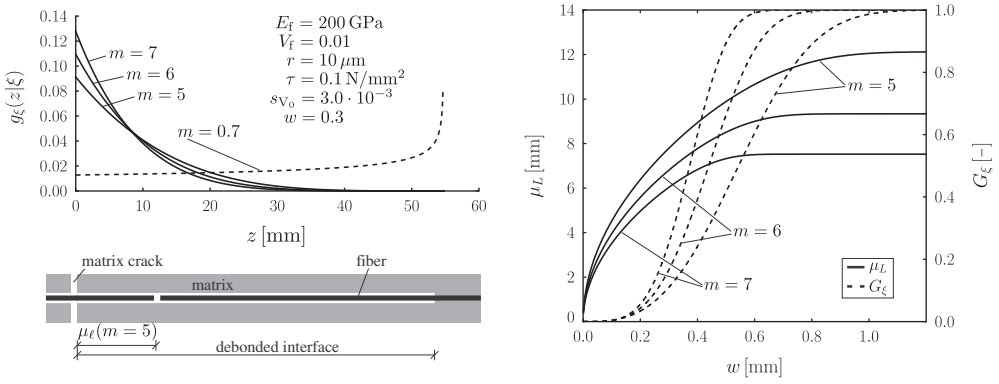

Fig. A.11. Probability density functions for fiber break position (left); mean pull-out lengths and corresponding fiber break probabilities (right).

this yields

$$k - \frac{k^{m+2} m w^{\star\frac{m+1}{2}}}{\varepsilon_0^{m+1}} = 0 \tag{B.4}$$

and therefore

$$w^\star = \frac{E_f}{T}\varepsilon_0^2 m^{-\frac{2}{m+1}}. \tag{B.5}$$

Appendix C. Fiber-in-composite breaking strain distribution

The assumption of random fiber breaking strain is based on the fact that brittle fibers are flaw-sensitive and the flaws can be assigned a value of strain to failure, which is a random variable. The applied strain shall be denoted as ε and the strain to failure distribution of the flaws $F(\varepsilon)$.

C.1. General Weibull distribution form

We consider the uniaxial tensile strain state since it is relevant for brittle fibers subjected to tensile loading. Given that reaching the strain to failure of either of the flaws leads to the ultimate failure of the structure and, that the number of flaws N in the volume of the structure is large, the distribution of strain to failure of the structure $G(\varepsilon)$ can be described by the weakest link model [28,45]. For a constant tensile strain throughout the whole structure, the strain to failure is defined as the minimum extreme of the parent distribution $F(\varepsilon)$

$$G(\varepsilon) = 1 - [1 - F(\varepsilon)]^N = 1 - \exp\left(N \ln[1 - F(\varepsilon)]\right) \tag{C.1}$$

Provided that $F(\varepsilon)$ has a lower bound ε_u and its left tail can be approximated by $C_0(\varepsilon - \varepsilon_u)^m$, $G(\varepsilon)$ has (for large N) the form

$$G(\varepsilon) = 1 - \exp\left[-NC_0(\varepsilon - \varepsilon_u)^m\right] \tag{C.2}$$

which is known from the work of Weibull [45]. Weibull expressed the distribution in the form

$$G(\varepsilon) = 1 - \exp\left[-\frac{V}{V_0}\left(\frac{\varepsilon - \varepsilon_u}{\varepsilon_{V_0}}\right)^m\right] \tag{C.3}$$

where V is the total structure volume and ε_{V_0} is the Weibull scale parameter corresponding to the reference unit V_0.

In general, the total volume V can be subdivided into a series of n units ΔV which are subjected to a variable strain ε_i with $i = 1, 2, \ldots, n$. Assuming that the strain state within the structure is uniquely defined by a reference strain ε_{ref}, it can be described as $\varepsilon_i(\varepsilon_{ref}, z_i)$, where z_i is the coordinate of ε_i. Given further, that the flaw strain to failure distribution $F(\varepsilon)$ is bounded at zero, the two parameter form of the Weibull distribution for the strain to failure of the structure reads

$$G(\varepsilon_{ref}) = 1 - \exp\left[-\sum_{i=1}^{n}\frac{\Delta V}{V_0}\left(\frac{\varepsilon_i(\varepsilon_{ref}, z_i)}{\varepsilon_{V_0}}\right)^m\right] \tag{C.4}$$

and as the size of ΔV approaches zero from above, the notation for the continuous form becomes

$$G(\varepsilon_{ref}) = 1 - \exp\left[-\int_V \frac{dV}{V_0}\left(\frac{\varepsilon(\varepsilon_{ref}, z)}{\varepsilon_{V_0}}\right)^m\right]. \tag{C.5}$$

The shape of the distribution is controlled by the Weibull modulus m and the scale by the scale parameter ε_{V_0} corresponding to the reference volume V_0.

C.2. Application to fibers

Let us now apply the strength distribution to a single fiber with longitudinal strain ε as a function of the fiber axis z. Since the strain is assumed constant within the cross-section, we can reduce the two dimensions in the fiber's cross-section plane by pre-solving the integral in the general Eq. (C.5) and thus obtain the integration in the fiber's longitudinal direction

$$G(\varepsilon_{ref}) = 1 - \exp\left[-\int_L \frac{\pi r^2 dz}{V_0}\left(\frac{\varepsilon(\varepsilon_{ref}, z)}{\varepsilon_{V_0}}\right)^m\right]. \tag{C.6}$$

Note, that this approach considers only production flaws related to the material volume. Another source of flaws on the surface with a different distribution might also be relevant for the fiber breaking strain but we neglect this effect here. These modifications would not affect the general form of the procedure derived below.

In the particular case of fibers in a composite with constant frictional stress τ at the fiber–matrix interface which is activated along the debonded length a, the fiber strain is a linear function of z (Eq. (4)) and can be uniquely described by its maximum value at the crack plane. We denote the resulting distribution G_ξ and refer to it as the fiber breaking strain distribution. The peak fiber strain is denoted as ξ – the fiber breaking strain – and the corresponding debonded length as a_ξ given by Eq. (12). Eq. (C.6) with this notation becomes

$$G_\xi(\xi) = 1 - \exp\left[-\int_{-a_\xi}^{a_\xi}\frac{\pi r^2 dz}{V_0}\left(\frac{\xi - Tz/E_f}{\varepsilon_{V_0}}\right)^m\right]. \tag{C.7}$$

Solving the integral and substituting Eq. (12) for a_ξ, we obtain the distribution function with the argument ξ in the two parameter Weibull form

$$G_\xi(\xi) = 1 - \exp\left[-\left(\frac{\xi}{\varepsilon_0}\right)^{m+1}\right] \tag{C.8}$$

with the scale parameter

$$\varepsilon_0 = \left(\frac{T(m+1)\varepsilon_{V_0}^m V_0}{2E_f \pi r^2}\right)^{1/(m+1)} \tag{C.9}$$

Differentiating Eq. (23) with respect to ξ gives the density function of the fiber breaking strain as

$$g_\xi(\xi) = \frac{\partial G_\xi(\xi)}{\partial \xi} = \frac{m+1}{\varepsilon_0}\left(\frac{\xi}{\varepsilon_0}\right)^m [1 - G_\xi(\xi)] \tag{C.10}$$

References

[1] Aveston J, Cooper G, Kelly A, Single, fracture multiple. the properties of fibre composites. In: Proc conf national physical laboratories. London: IPC Science and Technology Press Ltd.; 1971. p. 15–24.
[2] Aveston J, Kelly A. Theory of multiple fracture of fibrous composites. J Mater Sci 1973;8:411–61.
[3] Chudoba R, Sadílek V, Rypl R, Vořechovský M. Using python for scientific computing: efficient and flexible evaluation of the statistical characteristics of functions with multivariate random inputs. Comput Phys Commun 2013;184(2):414–27.
[4] Chudoba R, Vořechovský M, Konrad M. Stochastic modeling of multifilament yarns. I. Random properties within the cross-section and size effect. Int J Solids Struct 2006;43(3–4):413–34.
[5] Coleman BD. On the strength of classical fibres and fibre bundles. J Mech Phys Solids 1958;7:60–70.
[6] Cox HL. The elasticity and strength of paper and other fibrous materials. Brit J Appl Phys 1952;3:72–9.
[7] Curtin WA. Exact theory of fiber fragmentation in a single-filament composite. J Mater Sci 1991;26:5239–53.
[8] Curtin WA. Fiber pull-out and strain localization in ceramic matrix composites. J Mech Phys Solids 1993;41(1):35–53.
[9] Curtin WA. The tough to brittle transition in brittle matrix composites. J Mech Phys Solids 1993;41(2):217–45.
[10] Curtin WA, Ahn BK, Takeda N. Modeling brittle and tough stress–strain behavior in unidirectional ceramic matrix composites. Acta Mater 1998;46(10):3409–20.
[11] Daniels HE. The statistical theory of the strength of bundles of threads. I. Proceedings of the Royal Society of London. Series A. Math Phys Sci 1945;183(995):405–35.
[12] Daniels HE. The maximum of a gaussian process whose mean path has a maximum, with an application to the strength of bundles of fibres. Adv Appl Probab 1989;21(2):315.
[13] Dwaikat MMS, Spitas C, Spitas V. Effect of the stochastic nature of the constituents parameters on the predictability of the elastic properties of fibrous nano-composites. Compos Sci Technol 2012;72(15):1882–91.
[14] Evans AG, Zok FW. The physics and mechanics of fiber-reinforced brittle-matrix composites. J Mater Sci 1994;29(15):3857–96.
[15] Fantilli AP, Mihashi H, Vallini P. Multiple cracking and strain hardening in fiber reinforced concrete under uniaxial tension. Cement Concr Res 2009;39:1217–29.
[16] Harlow DG, Phoenix SL. The chain-of-bundles probability model for the strength of fibrous materials. II: A numerical study of convergence. J Compos Mater 1978;12(3):314–34.
[17] Harlow DG, Phoenix SL. Bounds on the probability of failure of composite materials. Int J Fract 1979;15(4):321–36.
[18] Harlow DG, Smith RL, Taylor HM. Lower tail analysis of the distribution of the strength of load-sharing systems. J Appl Probab 1983;20(2):358–67.
[19] Hegger J, Voss S. Investigations on the bearing behaviour and application potential of textile reinforced concrete. Eng Struct 2008;30(7):2050–6.
[20] Henstenburg RB, Phoenix SL. Interfacial shear strength studies using the single-filament-composite test. Part II: A probability model and Monte Carlo simulation. Polym Compos 1989;10(5):389–408.
[21] Hui C-Y, Phoenix SL, Ibnabdeljalil M, Smith RL. An exact closed form solution for fragmentation of Weibull fibers in a single filament composite with applications to fiber-reinforced ceramics. J Mech Phys Solids 1995;43(10):1551–85.
[22] Ibnabdeljalil M, Curtin WA. Strength and reliability of fiber-reinforced composites: localized load-sharing and associated size effects. Int J Solids Struct 1997;34(21):2649–68.
[23] P. Kabele, Mechanics of solids with cracks, CTU Prague, Department of Structural Mechanics; 2001.
[24] Kushch VI, Shmegera SV, Mishnaevsky Jr L. Explicit modeling the progressive interface damage in fibrous composite: analytical vs. numerical approach. Compos Sci Technol 2011;71(7):989–97.
[25] Li VC. A simplified micromechanical model of compressive strength of fiber-reinforced cementitious composites. Cement Concr Compos 1992;14:131–41.
[26] Marshall DB, Evans AG. Failure mechanisms in ceramic–fiber ceramic–matrix composites. J Am Ceram Soc 1985;68(5).
[27] Nairn JA. On the use of shear-lag methods for analysis of stress transfer in unidirectional composites. Mech Mater 1997;26(2):63–80.
[28] Oh H, Finnie I. On location of fracture in brittle solids. 1. Due to static loading. Int J Fract Mech 1970;6(3):287–300.
[29] Okabe T, Takeda N, Kamoshida Y, Shimizu M, Curtin WA. A 3D shear-lag model considering micro-damage and statistical strength prediction of unidirectional fiber-reinforced composites. Compos Sci Technol 2001;61(12):1773–87.
[30] Pan N. Prediction of statistical strengths of twisted fibre structures. J Mater Sci 1993:6107–14.
[31] Phoenix SL. Statistical theory for the strength of twisted fiber bundles with applications to yarns and cables. Text Res J 1979;49:407–23.
[32] Phoenix SL, Ibnabdeljalil M, Hui CY. Size effects in the distribution for strength of brittle matrix fibrous composites. Int J Solids Struct 1997;34(5):545–68.
[33] Phoenix SL. Probabilistic strength analysis of fibre bundle structures. Fibre Sci Technol 1974;7:15–30.
[34] Phoenix SL. Statistical issues in the fracture of brittle-matrix fibrous composites. Compos Sci Technol 1993;48(1–4):65–80.
[35] Phoenix SL, Raj R. Scalings in fracture probabilities for a brittle matrix fiber composite. Acta Metall Mater 1992;40(11):2813–28.
[36] Phoenix SL, Taylor HM. The asymptotic strength distribution of a general fiber bundle. Adv Appl Probab 1973;5:200–16.
[37] Scholzen A, Chudoba R, Hegger J. Dünnwandiges Schalentragwerk aus textilbewehrtem Beton. Beton Stahlbeton 2012;107(11):767–76.
[38] Smith LR, Phoenix LS. Asymptotic distributions for the failure of fibrous materials under series-parallel structure and equal load-sharing. J Appl Mech 1981;48:75–82.
[39] Smith RL. The asymptotic distribution of the strength of a series-parallel system with equal load-sharing. Anna Probab 1982;10(1):137–71.
[40] Swolfs Y, Gorbatikh L, Romanov V, Orlova S, Lomov SV, Verpoest I. Stress concentrations in an impregnated fibre bundle with random fibre packing. Compos Sci Technol 2013;74:113–20.
[41] Thouless M, Evans A. Effects of pull-out on the mechanical-properties of ceramic–matrix composites. Acta Metall 1988;36(3):517–22.
[42] Vaughan TJ, McCarthy CT. Micromechanical modelling of the transverse damage behaviour in fibre reinforced composites. Compos Sci Technol 2011;71(3):388–96.
[43] Vořechovský M, Sadílek V, Rypl R. Probabilistic evaluation of crack bridge performance in fiber reinforced composites. Eng Mech 2013;20(1):3–11.
[44] Vořechovský M, Chudoba R. Stochastic modeling of multifilament yarns: II. Random properties over the length and size effect. Int J Solids Struct 2006;43(3–4):435–58.
[45] Weibull W. The phenomenon of rupture in solids. Roy Swedish Inst Eng Res (Ingenioersvetenskaps Akad Handl) 1939;153:1–55.
[46] Weichold O, Hojczyk M. Size effects in multifilament glass-rovings: the influence of geometrical factors on their performance in textile-reinforced concrete. Text Res J 2009;79(16):1438–45.
[47] Xia Z, Curtin WA, Okabe T. Green's function vs. shear-lag models of damage and failure in fiber composites. Compos Sci Technol 2002;62(10–11):1279–88.
[48] Xia Z, Curtin WA, Peters PWM. Multiscale modeling of failure in metal matrix composites. Acta Mater 2001;49(2):273–87.
[49] Xia Z, Curtin WA. Tough-to-brittle transitions in ceramic–matrix composites with increasing interfacial shear stress. Acta Mater 2000;48(20):4879–92.
[50] Xia Z, Okabe T, Curtin WA. Shear-lag versus finite element models for stress transfer in fiber-reinforced composites. Compos Sci Technol 2002;62(9):1141–9.
[51] Zhandarov S, Mäder E. Characterization of fiber/matrix interface strength: applicability of different tests, approaches and parameters. Compos Sci Technol 2005;65(1):149–60.

Composites Science and Technology 90 (2014) 209

Contents lists available at ScienceDirect

Composites Science and Technology

journal homepage: www.elsevier.com/locate/compscitech

Corrigendum

Corrigendum to 'Brittle matrix composites with heterogeneous reinforcement: Multi-scale model of a crack bridge with rigid matrix' [Composi. Sci. Technol. 89 (2013) 98–109]

R. Rypl [a,*], R. Chudoba [a], A. Scholzen [a], M. Vořechovský [b]

[a] Institute of Structural Concrete, RWTH Aachen University, Germany
[b] Institute of Structural Mechanics, Brno University of Technology, Czech Republic

The authors regret that is a mistake in the following equation in the article as mentioned below: p. 102, Eq. (43). The following equation:

$$w^{\star}_{\xi}(\tau) \propto \tau^{-1/(m+1)}$$

should be changed to

$$w^{\star}_{\xi}(\tau) \propto \tau^{(1-m)/(1+m)}.$$

The diagrams in Fig. 5 depicting this scaling are evaluated correctly but there is are some mistakes in the notation of the slopes. The correct slopes are marked by bolface letters in the corrected Fig. 5 below.

The authors would like to apologise for any inconvenience caused.

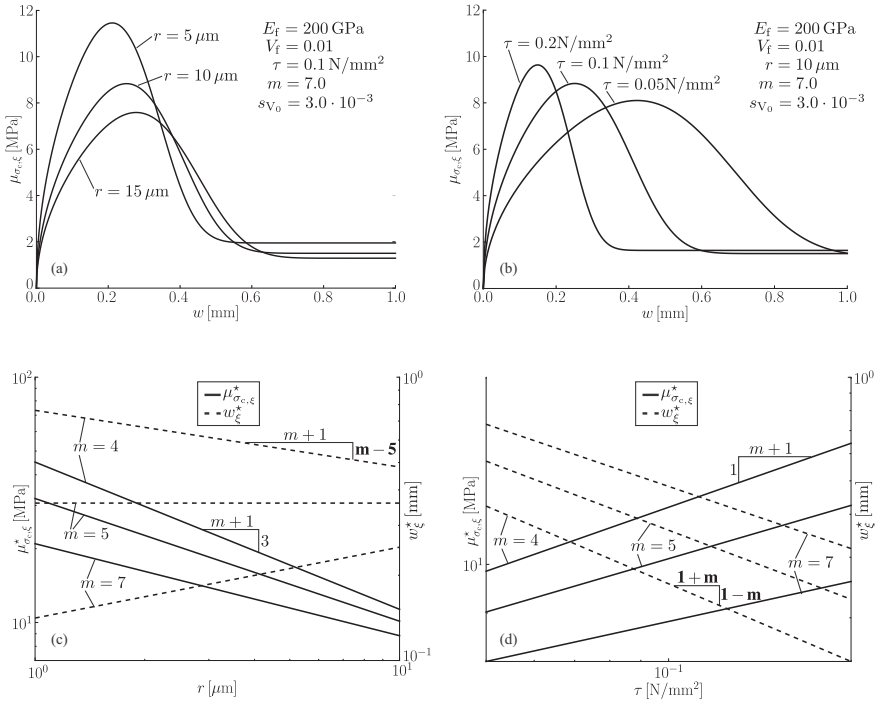

Fig. 5.

DOI of original article: http://dx.doi.org/10.1016/j.compscitech.2013.09.014
* Corresponding author. Tel.: +49 (0)241/80 25 172; fax: +49 (0)241/80 22 335.
E-mail address: rrypl@imb.rwth-aachen.de (R. Rypl).

0266-3538/$ - see front matter
http://dx.doi.org/.2013.12.005